Inorg. Chem. **2007**, *46*, 5967−5978

Manganese(III) Schiff Base Complexes: Chemistry Relevant to the Copolymerization of Epoxides and Carbon Dioxide

Donald J. Darensbourg* and Eric B. Frantz

Department of Chemistry, Texas A&M University, College Station, Texas 77843

Received March 1, 2007

Schiff base complexes of the form (acacen)$Mn^{III}X$ (acacen = *N,N*′-bis(acetylacetone)-1,2-ethylenediimine), where X = OAc, Cl, or N_3, have been evaluated for their ability to couple CO_2 and cyclohexene oxide in the presence of a variety of cocatalysts to provide cyclic or polycarbonates. These complexes proved to be ineffective at catalyzing this process; however, valuable information related to the coordination chemistry of these manganese Schiff bases was elucidated. Of importance, mechanistic findings as revealed by comprehensive studies involving structurally related (salen)CrX and (salen)CoX complexes strongly support the requirement of six-coordinate metal species for the effective copolymerization of CO_2 and epoxides. In the case of these Mn(III) complexes, it was determined that in chloroform or toluene solution a five-coordinate species was greatly favored over a six-coordinate species even in the presence of 20 equiv or more of various Lewis bases. Significantly epoxide monomers such as propylene oxide and cyclohexene oxide displayed no tendency to bind to these (acacen)MnX derivatives, even when used as solvents. Only in the case of excessive quantities of heterocyclic amines such as pyridine, DMAP, and DBU was spectral evidence of a six-coordinate Mn derivative observed in solution. X-ray crystal structures are provided for many of the complexes involved in this study, including the one-dimensional polymeric structures of [(acacen)$MnOAc\cdot 2H_2O]_n$, [(acacen)$MnN_3]_n$ ($\mu_{1,3}$-N_3), and a rare mixed bridging species [(acacen)$MnN_3]_n$ ($\mu_{1,3}$-N_3/$\mu_{1,1}$-N_3). In addition, a structure was obtained in which the unit cell contains both a (acacen)MnN_3(DMAP) and a (acacen)-MnN_3 species.

Introduction

The first catalysts capable of facilitating the copolymerization of CO_2 and epoxides appeared in the late 1960s beginning with Inoue's use of $ZnEt_2$ and H_2O to form poly(propylene carbonate) (PPC).[1] The general form of this process is given in eq 1. It is important to note here that in addition to the desired polycarbonate product, polyether linkages resulting from consecutive epoxide ring-opening and cyclic carbonate afforded from back-biting processes are often accompanying reactions. Over the next two decades, other heterogeneous catalyst systems appeared utilizing $ZnEt_2$, $Zn(OAc)_2$, $Zn(OH)_2$, and ZnO coupled with trihydric phenols and carboxylates of a wide variety.[2] The 1990s saw the advent and development of discrete Zn catalysts such as Darensbourg's bis(phenoxides) and Coates's β-diimine complexes.[3] These systems were more active toward the copolymerization of CO_2 and cyclohexene oxide (CHO) to give poly(cyclohexene carbonate) (PCHC), and in the case of the β-diimines, exceedingly high turnover frequencies upward

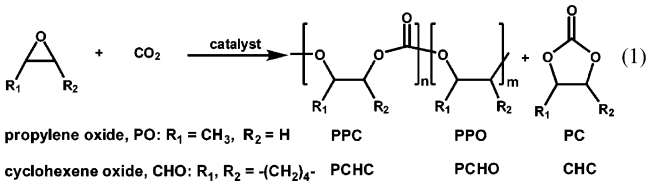

* To whom correspondence should be addressed. Fax: (979) 845-0158. E-mail: djdarens@mail.chem.tamu.edu.

(1) Inoue, S.; Kionuma, H.; Tsuruta, T. *J. Polym. Sci., Part B: Polym. Lett.* **1969**, *7*, 287−292.
(2) (a) Kuran, W.; Pasykiewicz, S.; Skupinska, J.; Rokicki, A. *Makromol. Chem.* **1976**, *177*, 11−20. (b) Kobayashi, M.; Inoue, S.; Tsuruta, T. *J. Polym. Sci., Polym. Chem. Ed.* **1973**, *11*, 2383−2385. (c) Soga, K.; Imai, E.; Hattori, I. *Polym. J.* **1981**, *13*, 407−410. (d) Motika, S. (Air Products and Chemicals, Inc., Acro Chemical Co., and Mitsui Petrochemical Industries Ltd.). U.S. Patent 5,026,676, 1991. (e) Gorecki, P.; Kuran, W. *J. Polym. Sci., Part C* **1985**, *23*, 299−304. (f) Ree, M.; Bae, J. Y.; Jung, J. H.; Shin, T. J. *J. Polym. Sci., Part A* **1999**, *37*, 1863−1876.
(3) (a) Darensbourg, D. J.; Holtcamp, M. W. *Macromolecules* **1995**, *28*, 7577−7579. (b) Cheng, M.; Lobkovsky, E. B.; Coates, G. W. *J. Am. Chem. Soc.* **1998**, *120*, 11018−11019.

10.1021/ic7003968 CCC: $37.00 © 2007 American Chemical Society
Published on Web 06/19/2007

of 1000 h^{-1} were obtained with PDI values as low as 1.08.[4] At the same time other active metal systems were under investigation including alkyl aluminum metalloporphyrins, chromium metalloporphyrins and $scCO_2$ soluble chromium metalloporphyrins.[5] The success of these chromium catalysts combined with a desire to synthesize stereo- and regioregular polycarbonates led to Darensbourg's application of chiral chromium salen complexes to the formation of PCHC and PPC.[6] This development was inspired by Jacobsen's advancements in the enantioselective ring-opening of epoxides by chromium salen.[7] It was found that, similar to the metalloporphyrins, the attainment of high activity required cocatalysts such as the Lewis bases, DMAP, *N*-MeIm, and Cy_3P or anionic salts such as PPN^+Cl^- or $PPN^+N_3^-$.[8] Although these binary catalytic systems did not lead to stereoregular polycarbonates, they do represent the most active metal salen catalysts to date for cyclohexene oxide with turnover frequencies of near 1200 h^{-1}, PDI values as low as 1.1, and >99% polycarbonate linkages. Most recently, Ding and co-workers have shown that dinuclear complexes of magnesium and zinc are effective at copolymerizing cyclohexene oxide and CO_2 under extremely mild reaction conditions.[9]

Significant steps in the direction of stereo- and regioregular poly(propylene carbonate) and stereoregular poly(cyclohexene carbonate) have been taken by the groups of Coates and Lu with the use of cobalt salen complexes of the form (*R,R*)-(salcy)CoX.[10] These complexes were developed by Jacobsen for the asymmetric hydrolytic kinetic resolution of terminal epoxides.[11] By variation of the apical ligand X and employment of anionic cocatalysts such as PPN^+Cl^- and $PPN^+OBzF_5^-$, Coates has been able to synthesize PPC with turnover frequencies of greater than 600 h^{-1} at mild reaction conditions (22 °C, 13.8 bar) and containing >90% head-to-tail linkages.[12] Isotactic, regioregular PPC is obtained with (*R,R*)-(salcy)CoBr starting from (*S*)-propylene oxide (PO) and syndio-enriched regioregular PPC is obtained from a reaction of *rac*-PO and *rac*-(salcy)CoBr. Lu has employed (*R,R*)-(salcy)Co($OC_6H_3(NO_2)_2$) and PPN^+Cl^- to achieve a turnover frequency of 1400 h^{-1} under moderate conditions (45 °C, 20 bar).[13] At room temperature and atmospheric pressure, the same catalyst with 2 equiv of MTBD (7-methyl-1,5,7-triazabicyclo[4.4.0]dec-5-ene) produced PPC with 96% head-to-tail linkages. Cobalt salen catalysts have also been applied to the formation of stereoregular PCHC. In the absence of a cocatalyst, (*R,R*)-(salcy)$CoOBzF_5$ at 22 °C and 55 bar produced polycarbonate with up to 76% *r*-centered tetrads with turnover frequencies of up to 93 h^{-1}.[14]

With the success of chromium and cobalt salen systems, the investigation of other suitable metals could potentially be valuable. Logically, other first role transition metals such as iron and manganese may hold some similar catalytic characteristics to chromium and cobalt. Darensbourg synthesized (salen)FeOPh and (salen)Fe(acac) in an effort to develop a series of iron salen catalysts.[15] However, these complexes failed to catalyze the formation of PCHC, yielding only trace amounts of cyclic carbonate. Manganese cyclen complexes have been applied to the synthesis of propylene carbonate (PC) and epichlorohydrin carbonate with [Mn(Me_4-cyclen)(NO_3)](ClO_4) being the most active for epichlorohydrin with a TOF of 449 h^{-1} under harsh conditions (120 °C, 6.9 bar).[16] Inoue has successfully applied the manganese porphyrin complex (tpp)MnOAc to the formation of PCHC under moderate conditions (80 °C, 51 bar) with a TOF of 16.3 h^{-1}.[17] This polymer had $M_n = 6700$, PDI = 1.3, and 99% carbonate linkages. The catalyst was not effective for the formation of PPC from propylene oxide and CO_2, producing only cyclic PC. Pertinent to our research, a manganese salen complex (salophen)MnOAc was applied to the copolymerization of CHO and CO_2 but only resulted in the formation of polyether.

Presented here is a fundamental study of the coordination chemistry of manganese Schiff base complexes as it relates to the copolymerization of CO_2 and epoxides. The ligand system selected for study is that of manganese acacen (acacen = *N,N′* −bis(acetylacetone)-1,2-ethylenediimine). These complexes are easily synthesized and exhibit a propensity to provide X-ray suitable crystals for structural analysis. Boucher and Day have prepared several of these complexes with a wide variety of axial ligands and provided magnetic susceptibility data.[18]

Each complex was characterized by X-ray crystallography (Scheme 1) and (excluding **2**) are presented here together with their extended macrostructures. A FT-IR study has been

(4) (a) Darensbourg, D. J.; Holtcamp, M. W.; Struck, G. E.; Zimmer, M. S.; Niezgoda, S. A.; Rainey, P.; Robertson, J. B.; Draper, J. D.; Reibenspies. J. H. *J. Am. Chem. Soc.* **1999**, *121*, 107−116. (b) Darensbourg, D. J.; Wildeson, J. R.; Yarbrough, J. C.; Reibenspies, J. H. *J. Am. Chem. Soc.* **2000**, *122*, 12487−12496. (c) Moore, D. R.; Cheng, M.; Lobkovsky, E. B.; Coates, G. W. *Angew. Chem., Int. Ed.* **2002**, *41*, 2599−2602.

(5) (a) Aida, T.; Ishikawa, M.; Inoue, S. *Macromolecules* **1986**, *19*, 8−13. (b) Kruper, W. J.; Dellar, D. V. *J. Org. Chem.* **1995**, *60*, 725−727. (c) Mang, S.; Cooper, A. I.; Colclough, M. E.; Chauhan, N.; Holmes, A. B. *Macromolecules* **2000**, *33*, 303−308.

(6) (a) Darensbourg, D. J.; Yarbrough, J. C. *J. Am. Chem. Soc.* **2002**, *124*, 6335−6342. (b) Darensbourg, D. J.; Phelps, A. L. *Inorg. Chem.* **2005**, *44*, 4622−4629.

(7) (a) Martinez, L. E.; Leighton, J. L.; Carste, D. H.; Jacobsen, E. N. *J. Am. Chem. Soc.* **1995**, *117*, 5897−5898. (b) Hansen, K. B.; Leighton, J. L.; Jacobsen, E. N. *J. Am. Chem. Soc.* **1996**, *118*, 10924−10925.

(8) Darensbourg, D. J.; Mackiewicz, R. M.; Phelps, A. L.; Billodeaux, D. R. *Acc. Chem. Res.* **2004**, *37*, 836−844.

(9) (a) Xiao, Y.; Wang, Z.; Ding, K. *Macromolecules* **2006**, *39*, 128−137. (b) Xiao, Y.; Wang, Z.; Ding, K. *Chem.—Eur. J.* **2005**, *11*, 3668−3678.

(10) (a) Qin, Z.; Thomas, C. M.; Lee, S.; Coates, G. W. *Angew. Chem., Int. Ed.* **2003**, *42*, 5484−5487. (b) Lu, X.-B.; Wang, Y. *Angew. Chem., Int. Ed.* **2004**, *43*, 3574−3577.

(11) Tokunaga. M.; Larrow, J. F.; Kakiuchi, F.; Jacobsen, E. N. *Science* **1997**, *277*, 936−938.

(12) Cohen, C. T.; Chu, T.; Coates, G. W. *J. Am. Chem. Soc.* **2005**, *127*, 10869−10878.

(13) Lu, X.-B.; Shi, L.; Wang, Y.-M.; Zhang, R.; Zhang, Y.-J.; Peng, X.-J.; Zhang, Z.-C.; Li, B. *J. Am. Chem. Soc.* **2006**, *128*, 1664−1674.

(14) Cohen, C. T.; Thomas, C. M.; Peretti, K. L.; Lobkovsky, E. B; Coates, G. W. *Dalton Trans.* **2006**, 237−249.

(15) Darensbourg, D. J.; Ortiz, C. G.; Billodeaux, D. R. *Inorg. Chim. Acta.* **2003**, *357*, 2143−2149.

(16) Srivastava, R.; Bennur, T. H.; Srinivas, D. *J. Mol. Catal.* **2005**, *226*, 199−205.

(17) Sugimoto, H.; Ohshima, H.; Inoue, S. *J. Polym. Sci., Part A* **2003**, *41*, 3549−3555.

(18) Boucher, L. J.; Day, V. W. *Inorg. Chem.* **1977**, *16*, 1360−1367.

Scheme 1. Summary of the Complexes Employed in This Study

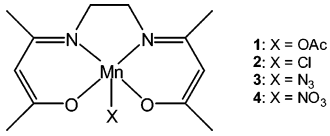

undertaken to evaluate the extent of these five-coordinate manganese species binding to various substrates of relevance to the copolymerization process. Fundamental difference in behavior between manganese and chromium Schiff base complexes will be described.

Experimental Section

Methods and Materials. Unless otherwise stated, all synthesis and manipulations discussed were carried out on a double-manifold Schlenk vacuum line under an argon atmosphere or in an argon-filled glovebox. Methanol, benzene, diethyl ether, dichloromethane, and pentane were freshly purified by a MBraun manual solvent purification system packed with Alcoa F200 activated alumina desiccant. Ethanol was freshly distilled from Mg/I_2. Cyclohexene oxide was purchased from TCI America and freshly distilled from CaH_2. Chloroform (EMD Chemicals Inc.), ethylenediamine (Aldrich), 2,4-pentanedione (Acros Organics), sodium azide (Lancaster Synthesis Inc.), 4-(dimethylamino)pyridine (DMAP, Aldrich), $AgNO_3$ (Spectrum Chemical Mgf. Corp.), 1,8-diazabicyclo[5.4.0]-undec-7-ene (DBU, Acros Organics), and $Mn(OAc)_3 \cdot 2H_2O$ (Strem Chemicals Inc.) were all used as received without further purification. Bone dry carbon dioxide was purchased from Scott Specialty Gases equipped with a liquid dip-tube.

The synthesis of *N*,*N*′-bis(acetylacetone)-1,2-ethylenediimine-[(acacen)H_2], [*N*,*N*′-bis(acetylacetone)-1,2-ethylenediimine]manganese(III) acetate diaqua [(acacen)MnOAc·$2H_2O$] (**1**·$2H_2O$), and [*N*,*N*′-bis(acetylacetone)-1,2-ethylenediimine]manganese(III) chloride [(acacen)MnCl] (**2**) were adapted from literature procedures.[18,19] An alternative route to the synthesis of [*N*,*N*′-bis(acetylacetone)-1,2-ethylenediimine]manganese(III) azide [(acacen)MnN_3] (**3**) employing $AgNO_3$ was developed and is reported. Elemental analysis was provided by the Rudiger Laufhutte Microanalysis Laboratory of the School of Chemical Sciences, University of Illinois, Urbana−Champaign. All infrared spectra were recorded using a Mattson 602 FT-IR spectrometer with DTGS and MCT detectors. All ^1H NMR were acquired using Unity+ 300 MHz and VXR 300 MHz superconducting NMR spectrometers.

Synthesis of *N*,*N*′-Bis(acetylacetone)-1,2-ethylenediimine-[(acacen)H_2]. A 125 mL three-necked round-bottom flask was charged with 25 g of 2,4-pentanedione (0.250 mol), along with a stir bar, placed in an oil bath, and equipped with a short-path distillation apparatus. To this flask was added, dropwise, 6.75 g of ethylenediamine (0.1125 mol) over the course of 10 min. At this point, the solution noticeably heated, and resultant water was seen to condense. After 30 min of stirring, the solution was slowly heated to 105 °C and reacted for 24 h. The resulting red-orange mixture was cooled to room temperature, and the crude off-white colored product was collected by filtration in air. The product was then dissolved in 250 mL of CH_2Cl_2, dried over 10 g of Na_2SO_4, and filtered. Solvent was removed in vacuo, and an off-white solid was obtained after it was recrystallized twice from a CH_2Cl_2/pentane mixture. Yield: 17.26 g (67.2%). ^1H NMR ($CDCl_3$, 300 MHz): δ 10.88 (s, 2H), 4.97 (s, 2H), 3.41 (t, 4H), 1.98 (s, 6H), 1.88 (s, 6H).

(19) McCarthy, P. J.; Hovey, R. J.; Ueno, K.; Martell, A. E. *Inorg. Chem.* **1955**, *77*, 5820−5824.

Synthesis of [*N*,*N*′-Bis(acetylacetone)-1,2-ethylenediimine]-manganese(III) Acetate Diaqua [(acacen)MnOAc·$2H_2O$] (1·$2H_2O$). A 125 mL Schlenk flask was charged with 0.2 g of acacenH_2 (0.892 mol), 0.2 g of $Mn(OAc)_3 \cdot 2H_2O$ (0.746 mol), and 25 mL of MeOH. This mixture was stirred under argon for 10 h. The MeOH was then removed in vacuo; 50 mL of distilled H_2O was added, and the solution was mixed for 1 h before the unreacted Mn was removed by filtration in air. The filtered solution was poured into a 500 mL separatory funnel, and the unreacted ligand was extracted with 50 mL of $CHCl_3$. The product was then isolated by removal of H_2O in vacuo, redissolved in 100 mL of CH_2Cl_2, and dried with 2 g of $MgSO_4$. The final product was isolated by removal of CH_2Cl_2 in vacuo with heat (60 °C) for 16 h to give 70 mg (25.1% yield) of a dark-brown microcrystalline powder. Single crystals suitable for X-ray diffraction were obtained by slow diffusion of pentane into a saturated CH_2Cl_2 solution of the complex. Anal. Calcd for $C_{14}H_{25}N_2O_6Mn$: C, 45.17; H, 6.77; N, 7.52. Found: C, 46.85; H, 6.69; N, 7.65.

Synthesis of [*N*,*N*′-Bis(acetylacetone)-1,2-ethylenediimine]-manganese(III) Chloride [(acacen)MnCl] (2). A 200 mL Schlenk flask was charged with 5 g of acacenH_2 (22.3 mmol), 5 g of $Mn(OAc)_3 \cdot 2H_2O$ (18.6 mmol), and 150 mL of MeOH. This mixture was stirred under argon for 18 h. The MeOH was then removed in vacuo; 200 mL of distilled H_2O was added, and the solution was mixed for 1 h before the unreacted Mn was removed by filtration in air. The filtered solution was poured into a 1000 mL separatory funnel, and the unreacted ligand was extracted with 200 mL of $CHCl_3$. The aqueous solution of (acacen)MnOAc was then treated with 50 g of NaCl and shaken vigorously. The product was then extracted with 5 × 200 mL of $CHCl_3$, separated from the aqueous phase, and reextracted from the organic phase with 200 mL of distilled H_2O. To this solution, 50 g of NaCl was added, and the mixture was shaken vigorously, followed by extraction of the product with 7 × 200 mL of $CHCl_3$. The solution was then reduced in volume to 250 mL *in vacuo* and dried with Na_2SO_4, followed by complete removal of solvent to isolated solid product. Recrystallization of the final product was obtained from 50 mL of benzene and 500 mL of diethyl ether. This yielded 3.28 g (56.4%) of a dark-brown microcrystalline powder.

Synthesis of [*N*,*N*′-Bis(acetylacetone)-1,2-ethylenediimine]-manganese(III) Azide [(acacen)MnN_3] (3). A 125 mL round-bottom flask was charged with 0.3 g of **2** (0.959 mmol), 0.178 g of $AgNO_3$ (1.06 mmol), and 30 mL of distilled H_2O. A heavy, white precipitant immediately formed and was filtered from the aqueous solution after 30 min of mixing. The solution was transferred to a 500 mL separatory funnel, treated with 6.5 g of NaN_3, and vigorously shaken. The product was extracted with 100 mL of $CHCl_3$, dried by Na_2SO_4, filtered, and rinsed with an additional 30 mL of $CHCl_3$. The solution volume was reduced to ∼15 mL in vacuo, and the final product was recrystallized by the addition of 300 mL of diethyl ether. A fine, dark brown microcrystalline solid was collected by filtration and dried in air. Yield: 146 mg (47.3%). Single crystals suitable for X-ray diffraction were obtained by slow diffusion of pentane into a saturated CH_2Cl_2 solution of the complex. Anal. Calcd for $C_{12}H_{18}N_5O_2Mn$: C, 45.15; H, 5.68; N, 21.94. Found: C, 44.62; H, 5.61; N, 21.19.

Synthesis of [*N*,*N*′-Bis(acetylacetone)-1,2-ethylenediimine]-manganese(III) Nitrate [(acacen)$MnNO_3$(EtOH)] (4). A 125 mL round-bottom flask was charged with 0.2 g of **2** (640 mmol), 0.12 g of $AgNO_3$ (704 mmol), and 25 mL of distilled H_2O. After 60 min of mixing, a heavy, white precipitant was removed by filtration. The final product was obtained by removal of H_2O in vacuo (24 h) and the azeotrope of benzene to give 153 mg (70.5%) of a fine

brown powder. Single crystals suitable for X-ray diffraction were obtained by slow diffusion of diethyl ether into a saturated EtOH solution of the complex.

Infrared Equilibrium and Binding Studies. Equilibrium studies were carried out by use of a Beer's Law plot by measuring absorption versus concentrations of **3** in chloroform at 0.0188, 0.015, 0.0113, 0.0108, and 0.0075 M. A 0.0188 M chloroform solution of **3** was then used in conjunction with 10, 12.5, 15, 17.5, and 20 equiv of DMAP to determine concentration of both five- and six-coordinate species under varying conditions. Binding studies with other cocatalysts were performed in a similar manner through the use of a 0.0188 M chloroform solution of **3** with varying equivalents (5 to 100) of the species under study.

Copolymerization Reactions. Polymerization experiments were performed using a 300 mL Parr autoclave reactor heated to 80 °C overnight while under vacuum. Reaction mixtures were prepared by dissolution of 50 mg of catalyst and an appropriate amount of cocatalyst in neat cyclohexene oxide, and then the mixture was added to the reactor by the injection port. Typical reactions were run at 80 °C under 35 bar of CO_2 pressure for 24 h. Following each reaction, the content of the reactor was dissolved in CH_2Cl_2 and analyzed by FT-IR to ascertain the presence of cyclic carbonate and polycarbonate.

X-ray Structural Studies. Single crystals of **3′**, **3″·(3·**DMAP**)**, and **3·**pyr suitable for X-ray diffraction were obtained by slow diffusion of pentane into an (acacen)MnN_3/CH_2Cl_2 solution containing 20 equiv of Ph_3P, 10 equiv of DMAP, and a solution of **3** in pyridine, respectively. For all reported structures, a Bausch and Lomb 10× microscope was used to identify suitable crystals of the same habit. Each crystal was coated in paratone, affixed to a Nylon loop, and placed under streaming nitrogen (110 K) in a Bruker SMART 1000 CCD or Bruker-D8 Adv GADDS diffractometer. Space group determination was made on the basis of systematic absences and intensity statistics. Crystal structures were solved by direct methods (for **3**, **3″·(3·**DMAP), and **3·**pyr) or DIRDIF (for **1·**$2H_2O$, **3′**, and **4·**EtOH) and refined by full-matrix least-squares on F^2. Except in the cases of water and ethanol, all H atoms were placed in idealized positions with fixed isotropic displacement parameters equal to 1.5 times (1.2 for methyl protons) the equivalent isotropic displacement parameters of the atom to which they are attached. Water and ethanol protons were located by Fourier difference maps. All non-hydrogen atoms were refined using anisotropic displacement parameters.

Programs used: data collection and cell refinement, SMART WNT/2000, version 5.632,[20] or FRAMBO, version 4.1.05 (GADDS);[21] data reductions, SAINTPLUS, version 6.63;[22] absorption correction, SADABS;[23] structural solutions, SHELXS-97,[24] DIRDIF-99.2,[25] and WinGX, version 1.70.01;[26] structural refinement, SHELXL-97;[27] graphics and publication materials, SHEXTL, version 6.14,[28] and X-Seed, version 1.5.[29]

Results and Discussion

Synthesis and Structural Characterization of (acacen)MnX Complexes. The synthesis of several five-coordinate square-pyramidal complexes of the general formula (acacen)MnX has been well-developed, thereby providing a reliable route to numerous derivatives.[18] The procedure reported, however, is rather cumbersome because it requires the formation of (acacen)MnCl (**2**) from (acacen)Mn(OAc) (**1**) which was previously isolated from the reaction of $Mn(OAc)_3$ and H_2acacen in water. That is, the recovery of (acacen)MnCl from the aqueous solution involves several extractions of the complex with copious quantities of chloroform. Furthermore, the anion exchange reaction of (acacen)MnCl with a NaX salt requires a multistep lengthy extraction processes. A more convenient preparation of the desired azide analog was achieved by the in situ formation of the intermediate (acacen)$MnNO_3$ (**4**) derivative by eq 2. Direct reaction of the aqueous solution of complex **4** with NaN_3, followed by a one-step extraction with a minimum quantity of chloroform, led to an acceptable yield (47.3%) of (acacen)MnN_3 (**3**). Presumably, this variation is a general method for the synthesis of (acacen)MnX derivatives from complex **4** and NaX.

$$\underset{\mathbf{2}}{\text{(acacen)MnCl}} + \text{AgNO}_3 \rightarrow \underset{\mathbf{4}}{\text{(acacen)MnNO}_3} + \text{AgCl}\downarrow \qquad (2)$$

Numerous examples of manganese(III) Schiff base complexes have been reported exhibiting both monomeric and extended polymeric coordination modes. In the former case, both five- and six-coordinate complexes have been crystallographically described, with (acacen)MnCl[18] and (bzacen)MnCl[30] (bzacen = *N*,*N*′-bis(benzoylacetone)-1,2-ethylenediimine) remaining five-coordinate. Six-coordinate complexes have been structurally characterized as both cations, for example, $[(bzacen)Mn(MeOH)_2]ClO_4$,[31] or neutral species such as (bzacen)Mn(NCS)(pyrimidine)[32] or (salphen)Mn(NCS)(MeOH).[33] One-dimensional polymeric coordination complexes resulting from five-coordinate square-pyramidal metal centers containing an apical ligand capable of forming a bridge to an adjacent molecule in the solid state which have been reported include (acacen)$MnN(CN)_2$,[34] (bzacen)MnOAc,[35] and (bzacen)MnN_3.[36] Other related Schiff base

(20) *SMART*, version 5.632; Bruker AXS Inc.: Madison, WI.
(21) *FRAMBO: FRAME Buffer Operation*, version 41.05; Bruker AXS Inc.: Madison, WI.
(22) *SAINT*, version 6.63; Bruker AXS Inc.: Madison, WI.
(23) Sheldrick, G. M. *SADABS, Program for Absorption Correction of Area Detector Frames*; Bruker AXS: Madison, WI.
(24) Sheldrick, G. *SHELXS-97, Program for Crystal Structure Solution*; Institüt für Anorganische Chemie der Universität: Gottingen, Germany, 1997.
(25) Beurskens, P.; Admiraal, G.; Beurskens, G.; Bosman, S.; Garicia-Granda, R.; Gould, J.; Smykalla, A.; Smykalla, C. *DIRDIF-99 Program System*; Technical Report for the Crystallography Laboratory; University of Nijimegen: Nijimegen, The Netherlands, 1999.
(26) Farrugia, L. J. *J. Appl. Cryst.* **1999**, *32*, 837−838.
(27) Sheldrick, G. *SHELXL-97, Program for Crystal Structure Refinement*; Institüt für Anorganische Chemie der Universität: Gottingen, Germany, 1997.
(28) Sheldrick, G. M. *SHELXTL*, version 6.14; Bruker-Nonius Inc.: Madison, WI, 2000.
(29) Barbour, L. J. X-Seed−A software tool for supramolecular crystallography. *J. Supramol. Chem.* **2001**, *1*, 189−191.
(30) Feng, Y.; Liu, S. *Acta Crystallogr.* **1996**, *52*, 2768−2770.
(31) Liu, S.; Feng, Y. *Polyhedron* **1996**, *15*, 4195−4201.
(32) Feng, Y. L.; Liu, S. X *J. Coord. Chem.* **1998**, *44*, 81−90.
(33) Zhou, Y.-Z.; Zheng, X.-F.; Han, D.; Zhang, H.-Y.; Shen, X.-Q.; Niu, C.-Y.; Chen, P.-K.; Hou, H.-W.; Zhu, Y. *Synth. React. Inorg. Metal−Org. Nano−Metal Chem.* **2006**, *36*, 693−699.
(34) Wang, S.-W.; Zhou, J.-H.; Li, B.-L.; Zhang, Y. *Chin. J. Inorg. Chem.* **2004**, *20*, 1433−1466.
(35) Haider, S. Z.; Hashem, A.; Khan, M. S.; Malik, K. M. A.; Hursthouse, M. B. *J. Bangladesh Acad. Sci.* **1985**, *9*, 105−112.
(36) Feng, Y. *Chin. J. Struct. Chem.* **2002**, *21*, 352−354.

Table 1. Crystallographic Data for (Acacen)MnX Derivatives

	1·2H_2O	**3**	**3′**	**4**·EtOH	**3″**·(**3**·DMAP)	**3**·Pyr
empirical formula	$C_{14}H_{24}MnN_2O_{5.5}$	$C_{12}H_{18}MnN_5O_2$	$C_{24}H_{36}Mn_2N_{10}O_4$	$C_{14}H_{24}MnN_3O_6$	$C_{31}H_{48}Mn_2N_{12}O_4$	$C_{17}H_{23}MnN_6O_2$
fw	363.29	319.25	638.51	385.30	762.69	398.35
temp (K)	110(2)	110(2)	110(2)	110(2)	110(2)	110(2)
cryst syst	monoclinic	monoclinic	orthorhombic	monoclinic	monoclinic	monoclinic
space group	*P*2/*c*	$P2_1/c$	*Pcan*	$P2_1/n$	$P2_1/c$	*P*2(1)
a (Å)	17.165(2)	10.2639(11)	13.778(10)	8.1727(5)	8.7824(9)	6.5564(5)
b (Å)	6.7320(9)	13.5749(15)	19.679(15)	17.1898(11)	13.9008(14)	14.10006(11)
c (Å)	14.886(2)	11.3173(11)	20.056(15)	12.3854(8)	28.352(3)	10.0027(8)
β (deg)	109.339(2)	112.173(6)		94.7680(10)	90.793(2)	93.029(4)
V (Å^3)	1623.1(4)	1460.2(3)	5438(7)	1733.97(19)	3461.0(6)	923.45(12)
D_{calcd} (g/cm^3)	1.487	1.452	1.560	1.476	1.464	1.433
Z	4	4	8	4	4	2
abs coeff (mm^{-1})	0.841	7.441	0.980	0.796	0.785	6.019
obsd relfns	10 674	10 112	36 076	16 375	19 090	7612
unique relfns [$I > 2\sigma(I)$]	2790	2238	4657	3952	6101	2707
restraints/params	12/209	0/185	204/361	0/222	0/452	1/239
GOF on F^2	1.058	1.004	1.022	0.989	1.057	1.005
R^a [$I > 2\sigma(I)$]	0.0557	0.0488	0.0793	0.0689	0.0497	0.0471
$R_w{}^b$ [$I > 2\sigma(I)$]	0.1361	0.1013	0.1902	0.1622	0.1231	0.0950

^{a} $R = \sum||F_o| - |F_c||/\sum|F_o|$. ^{b} $R_w = \{[\sum w(F_o^2 - F_c^2)^2]/[\sum w(F_o^2)^2]\}^{1/2}$, $w = 1/[\sigma^2(F_o^2) + (aP)^2 + bP]$, where $P = [\max(F_o^2),0) + 2(F_c^2)]/3$.

complexes exhibiting a similar propensity in the solid state are (salen)MnOAc,[37] (salpn)MnN_3,[38,39] and (2-OH-salpn)-MnOAc.[40] An azide-bridged polymer chain has also been reported for the $(acac)_2MnN_3$ derivative.[41] Crystallographic data pertaining to all complexes structurally characterized herein are provided in Table 1.

The X-ray structure of one member of the series of (acacen)MnX derivatives discussed herein, (acacen)MnCl (**2**), has previously been reported.[18] Crystals of the acetate (**1**) and azide (**3**) analogs suitable for X-ray diffraction were grown by the slow diffusion of pentane into a concentrated dichloromethane solution of the respective complexes. Perspective thermal ellipsoid drawings of (acacen)MnOAc·2H_2O and (acacen)MnN_3 are provided in Figures 1 and 2, along with a depiction of the resulting metal bridged polymeric chain. In each case, distortion of the ligand is presumed to be the results of steric interactions between bridged metal complexes. In **1·2H_2O** the acetates provide a near linear bridge between adjacent manganese centers with a Mn(1)−O(3)−O(4) bond angle of 171.12° (Table 2). This complex exhibits greater linearity than the same angle of 166.1° measured in (bzacen)MnOAc.[35] In addition, least-square plane calculations can be used to analyze ligand distortion by defining the three planes that compose the acacen complex, namely, the N_2O_2 plane and the two planes composed of O(1)−N(1)−C(1)−C(3) (ring 1) and O(2)−N(2)−C(4)−C(6) (ring 2). The dihedral angles between ring 1 and ring 2 and the N_2O_2 plane of **1**·2H_2O are 7.4 and 1.4°, respectively (Table 3). This is in contrast to the same dihedral angles measured in **3**, which were found to be 17.2 and 12.9°. In this instance, the bridging azides give a helical shape to

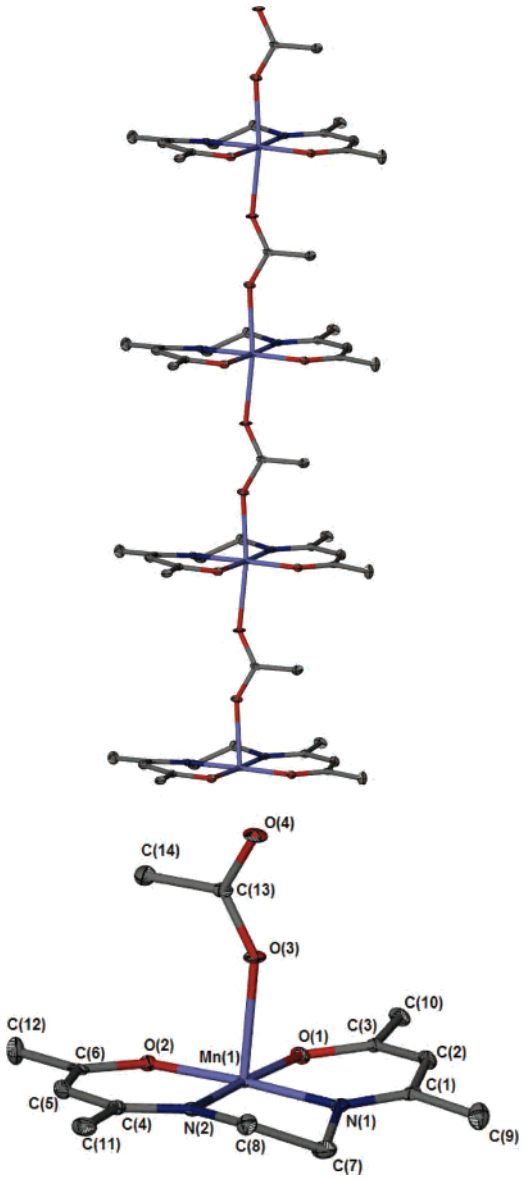

Figure 1. Thermal ellipsoid plot of **1**·2$H_2$0 at 50% probability. Waters are omitted for clarity. The polymer chain is represented as viewed along the *b*-axis.

(37) Davies, J. E.; Gatehouse, B. M.; Murray, K. S. *J. Chem. Soc., Dalton Trans.* **1973**, *22*, 2523−2527.
(38) Li, H.; Zhong, Z. J.; Duan, C.-Y.; You, X.-Z.; Mak, T. C. W.; Wu, B. *Inorg. Chim. Acta* **1998**, *271*, 99−104.
(39) Reddy, K. R.; Rajasekharan, M. V.; Tuchagues, J.-P. *Inorg. Chem.* **1998**, *37*, 5978−5982.
(40) Bonadies, J. A.; Kirk, M. L.; Lah, M. S.; Kessissoglou, D. P.; Hatfield, W. E.; Pecoraro, V. L. *Inorg. Chem.* **1989**, *28*, 2037−2044.
(41) Stults, B. R.; Marianelli, R. S.; Day, V. W. *Inorg. Chem.* **1975**, *14*, 722−730.

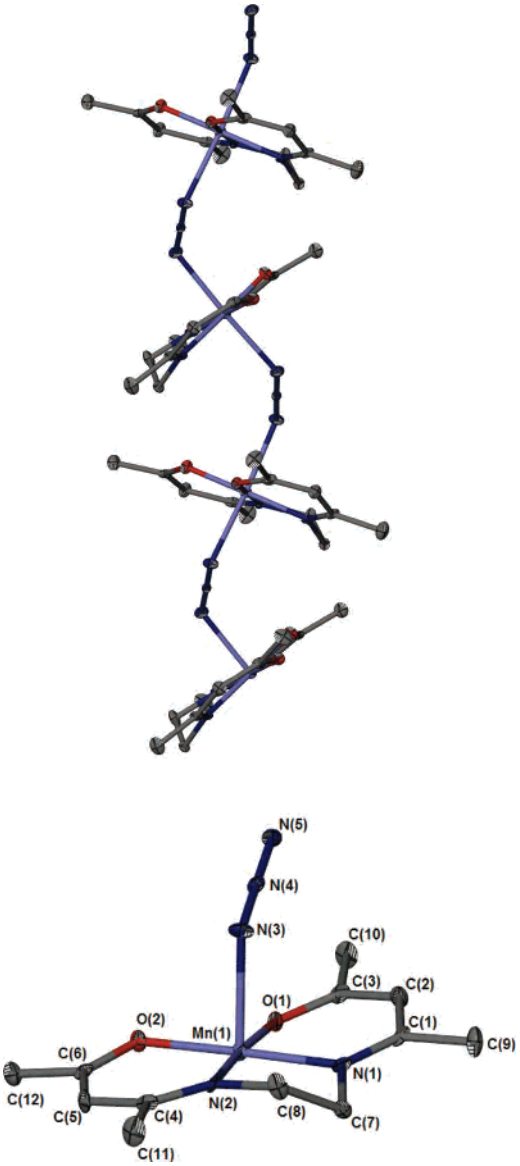

Figure 2. Thermal ellipsoid plot of **3** at 50% probability. The polymer chain is represented as viewed along the *c*-axis.

the metal ligand chain resulting from the metal−azide bond angles of 120.1 and 123.9° for Mn(1)−N(3)−N(4) and Mn(1)−N(4)−N(5), respectively. The helical shape assures a steric influence on adjacent complexes by pushing the rings of the ligand further out of plane from one another. Further indication of this can be seen from the buckling of the ethylene backbone as evidenced by an increase in distance of over 0.12 Å from the N_2O_2 plane for C(8) compared to that in **1**·2H_2O (Table 3).

Manganese displacement from the N_2O_2 plane is usually a function of coordinating ligands apical to the acacen moiety. In the case of **1**·2H_2O, the manganese oxygen bonds to the acetate ligands differs by 0.0474 Å, leading to a displacement of 0.0139 Å of the manganese atom out of the N_2O_2 plane. The addition of benzyl rings in [(bzacen)MnOAc]$_n$ derivative lowers this difference to 0.025 Å with no measurable displacement of the manganese from the coordination plane observed. In **3**, the manganese exhibits no measurable planar displacement, and the metal azide bond

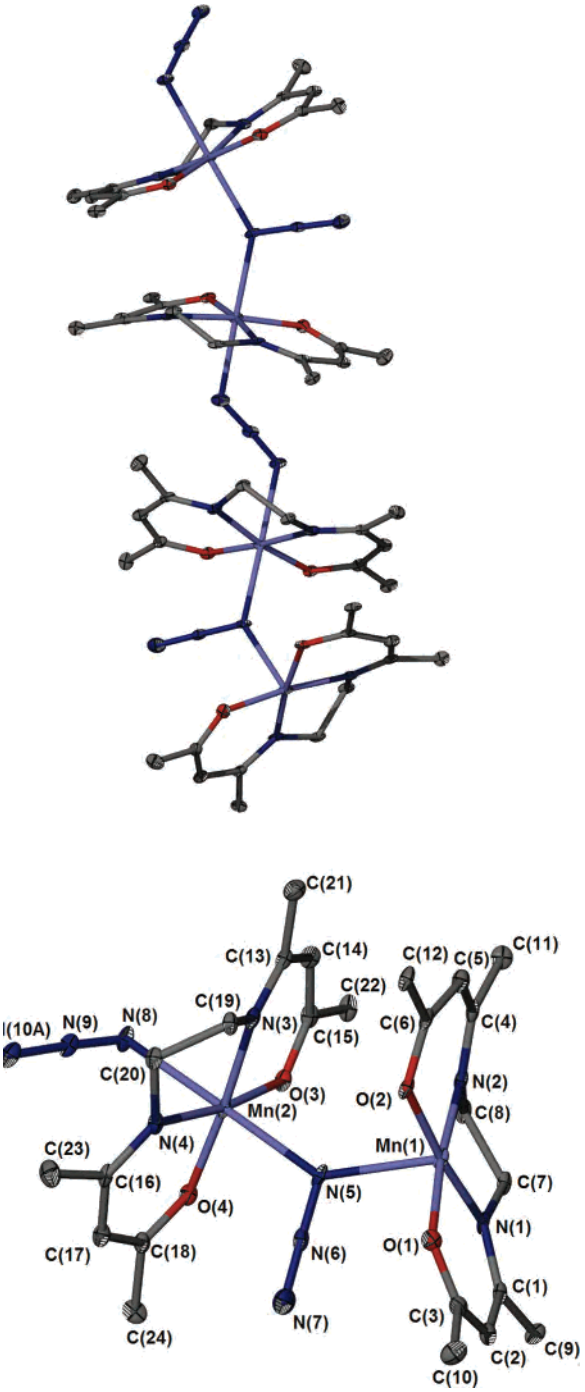

Figure 3. Thermal ellipsoid plot of **3′** at 50% probability. The polymer chain is represented as viewed along the *c*-axis.

lengths differ by only 0.015 Å. A greater metal displacement of 0.0695 Å is obtained with the addition of benzyl rings in [(bzacen)MnN_3]$_n$,[36] a complex which also forms a metal azide chain in a helical arrangement. In the structure of [(salpn)MnN_3]$_n$, the metal azide bond lengths differ by only 0.017 Å; however, the phenylate moieties of the salpn lie at 44° angle toward each other, consequently, forcing the manganese 0.0540 Å out of the N_2O_2 plane.[38,39]

In an attempt to isolate and characterize a six-coordinate derivative of (acacen)MnN_3 containing a phosphine ligand, crystals of complex **3′** were obtained from a CH_2Cl_2 solution of **3** in the presence of 20 equiv of triphenylphosphine.

Table 2. Selected Bond Distances and Angles for Complexes **1**·2H_2O, **3**, **3′**, **3″**·(**3**·DMAP), **4**·EtOH, and **3**·pyr

1·2H_2O

				N_2O_2 plane			
Mn(1)−O(1)	1.904(2)	Mn(1)−N(1)	1.977(3)	O(2)−Mn(1)−O(1)	91.71(10)	O(1)−Mn(1)−N(1)	91.77(11)
Mn(1)−O(2)	1.898(2)	Mn(1)−N(2)	1.985(3)	O(2)−Mn(1)−N(2)	92.62(11)	N(1)−Mn(1)−N(2)	83.92(12)
				acetate bridge			
Mn(1)−O(3)	2.2414(18)	Mn(1)−O(4)	2.2887(19)	O(1)−Mn(1)−O(3)	90.56(7)	Mn(1)−O(4)−C(13)	144.7(2)
				O(1)−Mn(1)−O(4)	88.96(7)	Mn(1)−O(3)−O(4)	171.25(9)
				Mn(1)−O(3)−C(13)	147.2(2)		
				metal-to-metal			
Mn−Mn (polymeric)	6.732						

3

				N_2O_2 plane			
Mn(1)−O(1)	1.909(3)	Mn(1)−N(1)	1.982(4)	O(2)−Mn(1)−O(1)	93.22(12)	O(1)−Mn(1)−N(1)	90.92(13)
Mn(1)−O(2)	1.917(3)	Mn(1)−N(2)	1.978(3)	O(2)−Mn(1)−N(2)	92.55(13)	N(1)−Mn(1)−N(2)	83.31(14)
				azide bridge ($\mu_{1,3}$)			
Mn(1)−N(3)	2.284(4)	Mn(1)−N(5)	2.299(4)	O(1)−Mn(1)−N(3)	87.95(13)	Mn(1)−N(3)−N(4)	120.2(3)
				O(1)−Mn(1)−N(5)	91.88(13)	Mn(1)−N(5)−N(4)	123.9(3)
				metal-to-metal			
Mn−Mn (polymeric)	5.664						

3′

				N_2O_2 plane			
Mn(1)−O(1)	1.921(5)	Mn(2)−O(3)	1.900(4)	O(2)−Mn(1)−O(1)	93.6(2)	O(4)−Mn(2)−O(3)	92.54(19)
Mn(1)−O(2)	1.901(4)	Mn(2)−O(4)	1.911(4)	O(2)−Mn(1)−N(2)	91.1(2)	O(4)−Mn(2)−N(4)	91.5(2)
Mn(1)−N(1)	1.978(5)	Mn(2)−N(3)	1.959(5)	O(1)−Mn(1)−N(1)	92.0(2)	O(3)−Mn(2)−N(3)	91.9(2)
				N(1)−Mn(1)−N(2)	83.1(2)	N(3)−Mn(2)−N(4)	83.9(2)
				azide bridge ($\mu_{1,3}/\mu_{1,1}$)			
Mn(1)−N(5)	2.326(5)	Mn(2)−N(8)	2.375(4)	O(1)−Mn(1)−N(5)	93.5(2)	O(3)−Mn(2)−N(8)	88.14(19)
Mn(2)−N(5)	2.328(5)	Mn(1)−N(10A)	2.320(6)	O(3)−Mn(2)−N(5)	92.40(19)	O(1)−Mn(1)−N(10A)	86.6(2)
				Mn(1)−N(5)−N(6)	110.6(4)	Mn(2)−N(8)−N(9)	114.9(4)
				Mn(2)−N(5)−N(6)	110.6(4)	Mn(1)−N(10A)−N(9)	128.6(5)
				Mn(1)−N(5)−Mn(2)	138.8(3)		
				metal-to-metal			
Mn(1)−Mn(1) (polymeric)	10.033	Mn(1)−Mn(2) (EE)	6.058				
Mn(1)−Mn(2) (EO)	4.356						

3·DMAP

				N_2O_2 plane			
Mn(1)−O(1)	1.9160(19)	Mn(1)−N(1)	1.966(2)	O(2)−Mn(1)−O(1)	92.27(8)	O(1)−Mn(1)−N(1)	91.84(9)
Mn(1)−O(2)	1.9226(18)	Mn(1)−N(2)	1.988(2)	O(2)−Mn(1)−N(2)	92.93(9)	N(1)−Mn(1)−N(2)	82.58(9)
				apical ligands			
Mn(1)−N(3)	2.214(3)	N(3)−N(4)	1.164(4)	O(1)−Mn(1)−N(3)	94.61(9)	O(1)−Mn(1)−N(6)	85.30(8)
Mn(1)−N(6)	2.388(2)	N(4)−N(5)	1.171(4)	Mn(1)−N(3)−N(4)	142.1(2)		

3″

				N_2O_2 plane			
Mn(2)−O(3)	1.8951(18)	Mn(2)−N(15)	1.972(2)	O(4)−Mn(2)−O(3)	88.83(8)	O(3)−Mn(2)−N(15)	91.42(8)
Mn(2)−O(4)	1.8952(19)	Mn(2)−N(16)	1.967(2)	O(4)−Mn(2)−N(16)	91.22(9)	N(15)−Mn(2)−N(16)	83.86(9)
				apical ligands			
Mn(2)−N(17)	2.084(2)	N(18)−N(19)	1.164(4)	O(3)−Mn(2)−N(17)	98.50(9)	Mn(2)−N(17)−N(18)	143.3(2)
N(17)−N(18)	1.175(3)						

4·EtOH

				N_2O_2 plane			
Mn(1)−O(1)	1.892(2)	Mn(1)−N(1)	1.973(2)	O(2)−Mn(1)−O(1)	91.45(9)	O(1)−Mn(1)−N(1)	92.76(9)
Mn(1)−O(2)	1.906(2)	Mn(1)−N(2)	1.965(2)	O(2)−Mn(1)−N(2)	91.34(9)	N(1)−Mn(1)−N(2)	84.48(10)
				apical ligands			
Mn(1)−O(3)	2.308(2)	N(3)−O(4)	1.258(3)	O(1)−Mn(1)−O(3)	95.56(8)	O(1)−Mn(1)−O(6)	89.15(8)
Mn(1)−O(6)	2.254(2)	N(3)−O(5)	1.232(3)	Mn(1)−O(3)−N(3)	134.01(19)	Mn(1)−O(6)−C(13)	120.44(18)
N(3)−O(3)	1.265(3)						

3·pyr

				N_2O_2 plane			
Mn(1)−O(1)	1.898(3)	Mn(1)−N(1)	1.986(4)	O(2)−Mn(1)−O(1)	91.03(15)	O(1)−Mn(1)−N(1)	92.75(16)
Mn(1)−O(2)	1.918(4)	Mn(1)−N(2)	1.962(4)	O(2)−Mn(1)−N(2)	92.14(16)	N(1)−Mn(1)−N(2)	83.52(18)
				apical ligands			
Mn(1)−N(3)	2.220(5)	N(3)−N(4)	1.193(6)	O(1)−Mn(1)−N(3)	92.05(16)	O(1)−Mn(1)−N(6)	87.72(15)
Mn(1)−N(6)	2.432(4)	N(4)−N(5)	1.168(6)	Mn(1)−N(3)−N(4)	127.3(4)		

Table 3. Selected Displacements and Dihedral Angles from the N_2O_2 Plane[a]

	Mn−N_2O_2 planar displacement (Å)	C(7)−N_2O_2 planar displacement (Å)	C(8)−N_2O_2 planar displacement (Å)	dihedral ring 1[b] to ring 2[b] (deg)	dihedral ring 1[b] to N_2O_2 plane (deg)	dihedral ring 2[b] to N_2O_2 plane (deg)
1·2H_2O	0.0139	−0.3893	0.1269	8.3	7.4	1.4
3	0.0000	−0.3888	0.2522	4.6	17.2	−12.9
3′ Mn(1)	0.0624	−0.0416	0.5021	22.4	−8.4	−30.8
3′ Mn(2)	0.068	−0.3900	0.284	22.2	16.1	7.1
3·DMAP	0.0785	0.5119	0.0270	27.0	−22.5	−4.5
3″	0.2755	−0.2247	0.2649	8.5	3.2	−11.3
4·EtOH	0.0138	−0.2420	0.3022	5.4	9.7	−15.1
3·pyr	0.0925	−0.0771	0.4457	29.8	−8.5	−21.3

[a] For least-square plane analysis, see Supporting Information. [b] Ring 1 = N(1)−O(1)−C(1)−C(3); ring 2 = N(2)−O(1)−C(4)−C(6).

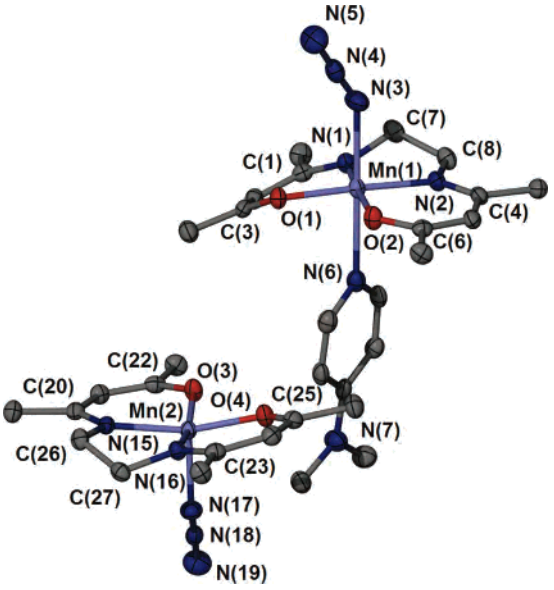

Figure 4. Thermal ellipsoid plots of **3**·DMAP and **3″**.

Complex **3′** was shown by X-ray crystallography to be a polymorph of **3** with a mixed coordination mode of $\mu_{1,1}/\mu_{1,3}$ bridging azides to form a polymer chain of $[((acacen)MnN_3)_2]_n$ (Figure 3). Such extended structures containing an end-on (EO) or end-to-end (EE) bridging azide have gained popularity recently because of their ferromagnetic properties, especially in the case of manganese(II) 1D and 3D chains.[42−45] The structure of **3′** represents a rare example of a manganese(III) chain of this type, and it may possess interesting magnetic properties. It can be seen from Figure 3 that the two acacen ligands of the asymmetric unit of **3′** are directed toward each other at an angle of 41.2° (from the Mn(1)−N(5)−Mn(2) angle of 138.8°) by the sp^2-hybridized nitrogen atom of the EO bridging azide. This leads to a 30.8° distortion of ring 2 from the Mn(1)N_2O_2 plane, the largest of any such distortion observed in this study. In an extended polymer structure, the repeating unit $((acacen)MnN_3)_2$ forms a helical pattern with its neighbor by being rotated by approximately 180° and returning to its original orientation every third repeating unit. The EO azide-bridged Mn(1)···Mn(2) separation is 4.356 Å and represents the closest metal−metal distance in any of the polymeric structures reported upon herein (Table 2).

As will be illustrated later in this report, we have demonstrated via solution binding studies monitored by infrared spectroscopy of complex **3** with various neutral and anionic donor ligands that an excess of DMAP ((4-dimethylamino)pyridine) reversibly coordinates to the manganese center (eq 3). Efforts were made to obtain suitable crystals of the six-coordinate (acacen)Mn(N_3)·DMAP complex for X-ray crystallographic characterization by layering pentane over a saturated chloroform solution of **3** and 10 equiv of DMAP. The resulting crystals were analyzed and shown to contain an asymmetric unit which included both six- and five-coordinate complexes, **3**·DMAP and **3″**, respectively (Figure 4). This finding is rather remarkable in that the two coexisting complexes found in the solid-state represent both derivatives involved in the equilibrium in eq 3 (vide infra).

$$(acacen)MnN_3 + DMAP \rightleftharpoons (acacen)Mn(N_3)\bullet DMAP \qquad (3)$$

Six-coordinate manganese derivatives containing heterocyclic amines as apical ligands have previously been structurally characterized, including (bzacen)Mn(NCS)(pyrimidine)[32] and (bzacen)Mn(NCS)(4,4′-bypiridine).[46,47] In the former complex, the manganese−pyrimidine bond distance of 2.504 Å is 0.307 Å longer than the Mn−NCS bond distance. This elongation is likely caused by the steric influence of the benzyl rings on the heterocyclic amine, contributing to the manganese atom displacement of 0.131 Å from the N_2O_2 plane. This metal displacement is greater than that seen of 0.0785 Å in **3**·DMAP (Table 3) where the difference in the two Mn−apical nitrogen bonds is 0.174 Å. The orientation of the ring system of DMAP and the three atom chain of the azide ligand runs along the bisection of the O(1)−Mn(1)−O(2) angle which may account for the saddle type distortion of the acacen rings.

The structure of **3″** is of interest because of the lack of a six ligand trans to the anion, and consequently, it is more akin to the species in solution. To our knowledge, the only other instances of coordinatively unsaturated manganese acacen complexes in the solid state are those previously mentioned, (acacen)MnCl and (bzacen)MnCl. The lack of

(42) Ray, U.; Jasimunddin, S.; Ghosh, B. K.; Monfort, M.; Ribas, J.; Mostafa, G.; Lu, T.-H.; Sinha, C. *Eur. J. Inorg. Chem.* **2004**, 250−259.
(43) Ghosh, A. K.; Ghoshal, D.; Zangrando, E.; Ribas, J.; Chaudhuri, N. R. *Inorg. Chem.* **2005**, *44*, 1786−1793.
(44) Bai, S.-Q.; Gao, E.-Q.; He, Z.; Fang, C.-F.; Yue, Y.-F.; Yan, C.-H. *Eur. J. Inorg. Chem.* **2006**, 407−415.
(45) Das, A.; Rosair, G. M.; El Fallah, M. S.; Ribas, J.; Mitra, S. *Inorg. Chem.* **2006**, *45*, 3301−3306.
(46) Liu, S. X.; Feng, Y. L. *Chem. J. Chin. Univ.* **1996**, *17*, 509−514.
(47) Feng, Y.; Liu, S. *Chin. J. Struct. Chem.* **1998**, *17*, 125−128.

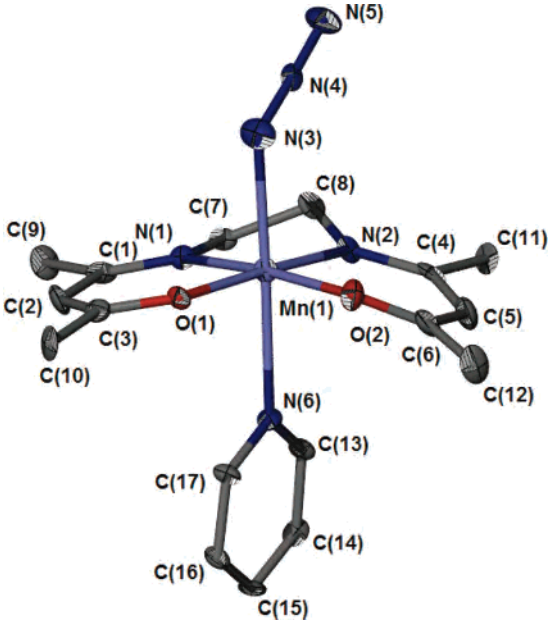

Figure 5. Thermal ellipsoid plot of **3**·pyr at 50% probability.

any steric demand from a six ligand is evident by the considerable out-of-plane displacement of the manganese atom from the N_2O_2 plane (Table 3). Of the three examples, (acacen)MnCl possesses the largest distance of 0.344 Å, followed by 0.304 Å for (bzacen)MnCl and 0.275 Å for **3**′′. In the former two cases, the acacen ligand holds a saddle shape where both of the acetyl imine rings are angled below the Mn−Cl bond (14.9/18.6° for acacen and 10.6/14.0° for bzacen). The azide complex, conversely, has a step-type arrangement where one ring (ring 1) is angled 3.2° toward the Mn−N_3 and the other (ring 2) 11.3° below. This is likely because of the close proximity of **3**·DMAP. The absence of a sixth ligand also removes any trans effect on the metal−azide bond and subsequently leads to a shortened manganese−nitrogen bond distance of 2.084 Å.

Infrared spectroscopic monitoring of the binding studies of complex **3** with pyridine also reveals the formation in chloroform of a six-coordinate manganese azide complex. X-ray quality crystals of (acacen)Mn(N_3)·pyridine (**3**·pyr) were obtained, and its structure was determined to be that depicted in Figure 5. As anticipated the structure of **3**·pyr bears numerous similarities to **3**·DMAP with the manganese displaced from the N_2O_2 plane by 0.0925 Å and a saddle-shaped acacen configuration with the ring dihedral angles of 8.5 and 21.3° below the coordination plane. Interestingly, both the azide and pyridine are closely oriented along the line N(2)−Mn(1)−O(1) which represents a nitrogen-rich plane of five nitrogen atoms. This coplanar relationship is also seen in **3**·DMAP where the azide and DMAP are oriented in much the same way.

Crystals of the synthetically useful intermediate (acacen)-$MnNO_3$ were grown by layering ether over a saturated solution of the complex in ethanol. A thermal ellipsoid representation of the ethanol adduct of (acacen)$MnNO_3$, complex **4**·EtOH, is provided in Figure 6. The structure of **4**·EtOH bears some resemblance to that of **1**·H_2O in that manganese forms an octahedral complex consisting of a N_2O_2

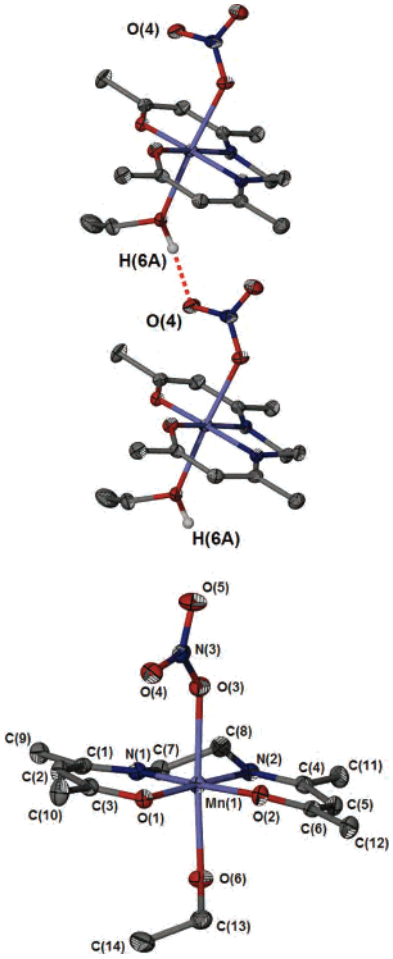

Figure 6. Thermal ellipsoid plot of **4**·EtOH at 50% probability. The hydrogen bond is viewed along the *a*-axis.

coordination plane and two axial ligands bound through oxygen atoms. This results in a nearly identical metal displacement from the N_2O_2 plane of 0.0138 Å, which can be attributed to a similar difference of 0.054 Å in the axial manganese−oxygen bond distances. Originally, we assumed that the nitrate anion would be non-coordinating, as seen in the perchlorate derivative, [(bzacen)Mn(MeOH)$_2$]ClO_4.[31] However, coordinated perchlorate and nitrite anions have been observed in the case of manganese bzacen complexes in the presence of methanol, ethanol, and acetonitrile.[48,49] Strong hydrogen bonding between the ethanol proton H(6A) and O(4) of the nitrate ligand leads to a chainlike solid-state structure with a hydrogen···acceptor distance of 1.84 Å.

Chemistry Pertinent to the Copolymerization of CO_2 and Epoxides in the Presence of Metal Schiff Base Catalysts. Complexes **1**, **2**, and **3** in the presence of 1 equiv of *n*-Bu_4NN_3 as a cocatalyst, following the common catalysis protocol (35 bar CO_2 and 80°), were ineffective at copolymerizing CO_2 and cyclohexene oxide.[50] These observations are in stark contrast to the highly active chromium and cobalt Schiff base catalyst systems.[9,10] In an effort to understand

(48) Xu, D.; Chen, B.; Chen, K.; Chen, C.; Miki, K.; Kasai, N. *Bull. Chem. Soc. Jpn.* **1989**, *62*, 2384.
(49) Feng, Y.; Liu, S. *Chem. J. Chin. Univ.* **2001**, *22*, 887−891.
(50) Trace quantities of the cyclic carbonate were afforded which are attributed to the cocatalysts, *n*-Bu_4NN_3.

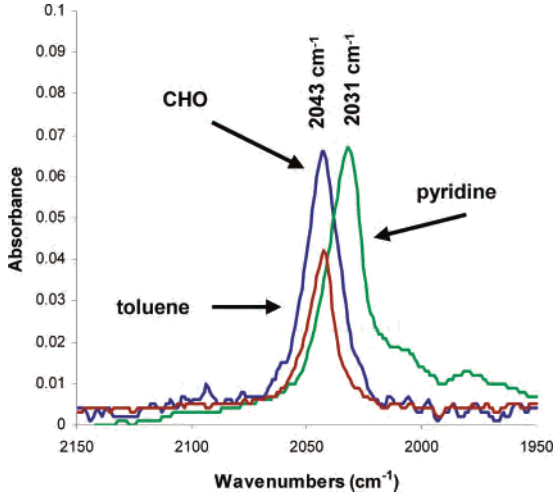

Figure 7. Spectra of **3** in toluene, cyclohexene oxide, and pyridine.

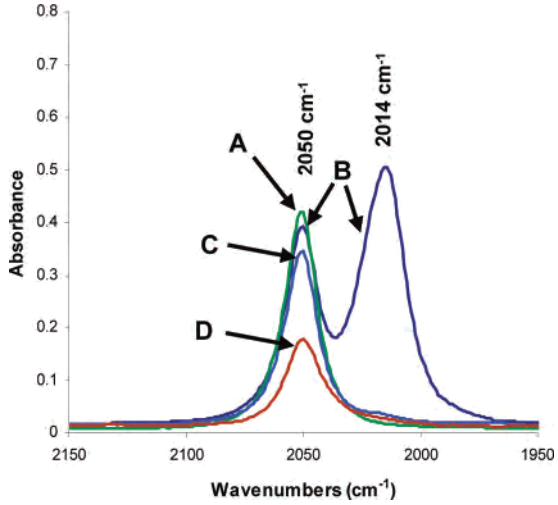

Figure 8. Spectra of chloroform solutions of **3** with (A) the five-coordinate manganese azide complex, (B) the five-coordinate complex with 1 equiv of "free" azide (from (n-Bu_4NN_3), and (C and D)) with 20 equiv of $(Cy)_3P$ and 100 equiv of n-Bu_3P, respectively.

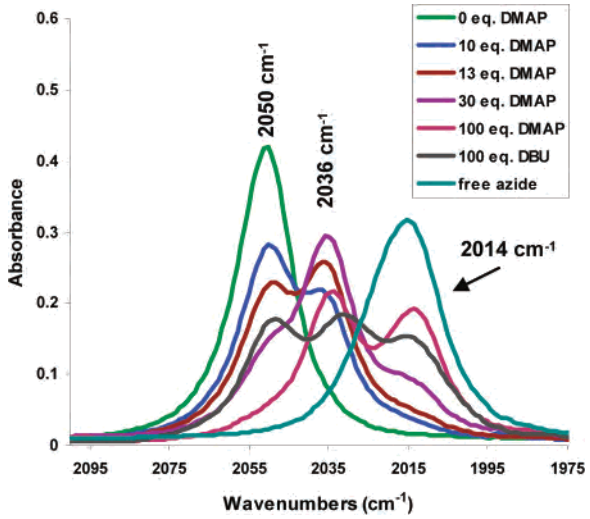

Figure 9. Spectra of chloroform solutions of **3** with varying concentration of DMAP and DBU. The stretches at 2050, 2036, and 2014 cm^{-1} represent five-coordinate, six-coordinate, and free azide species, respectively.

the cause of this difference between these closely related d^3 and d^4 transition metal systems, we have performed binding studies of a variety of ligands at the five-coordinate manganese center. To accomplish this we have employed the (acacen)MnN_3 derivative because the ν_{N3} stretching vibration is quite sensitive to coordination of a sixth ligand at the metal center.[8b,32] An inability of epoxides to bind to the metal center would greatly inhibit or prevent polymerization from occurring. *It should be noted here that a wide range of ligands, including weakly binding epoxides, readily coordinate to the metal center at equimolar concentrations in (salen)CrX derivatives.*

Figure 7 illustrates the ν_{N3} infrared spectrum of (acacen)-MnN_3 in the non-coordinating solvent toluene where its stretching mode occurs at 2043 cm^{-1}. Surprisingly, an identical ν_{N3} vibration is observed at 2043 cm^{-1} when complex **3** is dissolved in cyclohexene oxide. That is, even at this very high concentration of cyclohexene oxide, the manganese center remains coordinatively unsaturated. On the other hand, a six-coordinate manganese complex is observed with a ν_{N3} vibrational mode at 2031 cm^{-1} in the presence of the strongly coordinating pyridine ligand. The solid-state structure of this six-coordinate manganese derivative, **3**·pyr, was described earlier in this report.

Because of the limited solubility of complex **3** in toluene, it was desirable to change to an alternative, slightly more interacting solvent, chloroform to acquire quantitative binding data. In chloroform, the five-coordinate manganese azide ν_{N3} band in complex **3** occurs at 2050 cm^{-1}. The addition of 1 equiv of n-Bu_4NN_3 to **3** failed to result in the formation of a manganese diazide species as is seen with (salen)CrN_3.[51] However, two azide stretching modes are seen in the infrared spectrum of complex **3** in the presence of n-Bu_4NN_3, one resulting from, **3** and the other from the "free" azide anion (Figure 8). Phosphines display a similar disinclination to bind to the manganese center in **3**, although in this instance no spectroscopic evidence exists for the formation of a (salen)-$Cr(N_3)$·PR_3 complex.[51] The absence of the bulky substituted phenolate rings of salen in acacen could conceivably favor the binding of a bulky ligand such as tricyclohexylphosphine to **3**. However, as is readily seen in Figure 8, neither 20 equiv of Cy_3P nor 100 equiv of n-Bu_3P show any tendency to bind to complex **3**.

On the other hand, as previously demonstrated both in the solid-state and in solution, pyridine readily binds to complex **3**. Other heterocyclic amines such as DMAP and DBU were also found to coordinate to the manganese center in **3**. The binding of DMAP to complex **3** in chloroform solution proved to be an equilibrium process as depicted in eq 4, with equal quantities of the five-coordinate **3** (ν_{N3} = 2050 cm^{-1}) and six-coordinate **3**·DMAP (ν_{N3} = 2036 cm^{-1}) occurring at approximately 13.5 equiv of DMAP (Figure 9). *Recall that crystallization of this reaction mixture led to isolation of crystals containing* ***3***·*DMAP and* ***3*** *in the unit cell (vide supra).* The K_{eq} at ambient temperature was determined to be 3.07 ± 0.02 M^{-1} over the range of ~12.5 equiv of DMAP.

(51) (a) Darensbourg, D. J.; Mackiewicz, R. M. *J. Am. Chem. Soc.* **2005**, *127*, 14026−14038. (b) Darensbourg, D. J.; Mackiewicz, R. M.; Rodgers, J. L. *J. Am. Chem. Soc.* **2005**, *127*, 17565.

Scheme 2

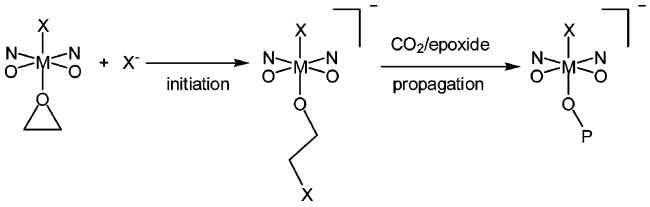

Beyond this concentration of DMAP, a second reaction occurs where the azide ligand is displaced from **3**·DMAP, resulting in formation of $[(acacen)Mn(DMAP)_2]N_3$. A similar phenomena was observed for the bicyclic amine DBU (Figure 9). However, the sterically more demanding DBU ligand requires a significantly more concentrated solution of amine to affect an extent of metal binding similar to that seen in the DMAP case.

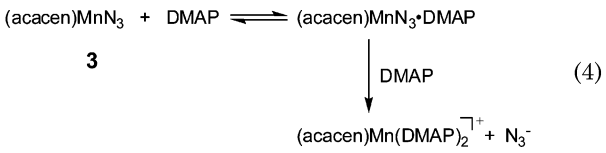

(4)

In the literature, there are a substantial number of mechanistic studies of the copolymerization of propylene oxide and cyclohexene oxide with carbon dioxide in the presence of chromium(III) and cobalt(III) salen catalysts.[6,7,9,10,12,13,51,52] The initiation of this process involves either a first- or second-order dependence on catalyst concentration. In either case, metal-binding of the epoxide activates the cyclic ether for ring-opening by an external nucleophile (as seen in Scheme 2) or a nucleophile on the (salen)MX catalyst. Propogation of the polymer chain involves the repeated formation of a carbonate anion by CO_2 insertion, followed by the ring-opening of an epoxide by the same anion. This process is facilitated by the presence of a ligand (cocatalyst) in the axial site trans to the growing polymer chain. That is, it is abundantly clear that a six-coordinate metal complex with a distorted octahedral geometry is necessary for copolymerization to proceed efficiently.

In light of the structural parameters presented herein and elsewhere, it is apparent that these (acacen)MnX complexes are directly related to their (salen)CrX analogs in that the acacen ligand bears a saddle or step shape with an axial ligand perpendicular to the N_2O_2 core. The open axial position is critical to the catalytic function of these structurally comparable metal derivatives because it represents an open site for substrate binding. For d^3 chromium(III) octahedral salen complexes, the t_{2g} orbitals are half-filled with the e_g antibonding orbitals unoccupied. Similarly, low spin d^6 octahedral cobalt(III) salen complexes possess filled t_{2g} orbitals with unoccupied e_g antibonding orbitals. Conversely, octahedral manganese(III) salen or acacen derivatives are d^4 and are known to be substantially labile because of Jahn−Teller distortion along the *z*-axis.[53] In the case of a high spin $S = 2$ configuration in distorted octahedral geometry, the degeneracy of the d_{z^2} and $d_{x^2-y^2}$ orbitals is broken with one unpaired electron occupying the d_{z^2} orbital. In square-pyramidal geometry, d_{z^2} and $d_{x^2-y^2}$ (orbitals) also lose degeneracy with the former dramatically decreased in energy (Figure 10). This leads to less distortion along the *z*-direction, making the five-coordinate complex more favorable.

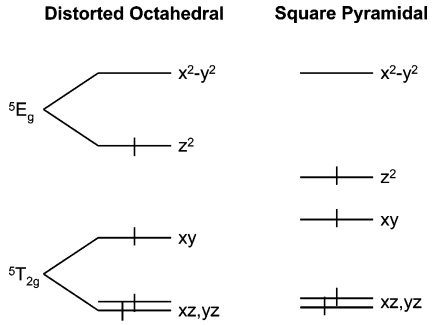

Figure 10. Theoretical ligand field splittings of d-orbitals for six- and five-coordinate Mn(III) complexes.

As a consequence of the ineffectiveness of five-coordinate Schiff base derivatives of Mn(III) to bind (activate) weakly coordinating epoxide ligands, thus forming distorted six-coordinate derivatives, these metal complexes are essentially incapable of ring-opening epoxides via either first- or second-order initiation processes.[54] In the rare instances when ring-opening does take place, insertion of a CO_2 molecule into the resulting Mn−OR is facilitated by the presence of a donor group trans to the manganese−oxygen moiety. In other words, an octahedral geometry is crucial to an efficient insertion process. Indeed, thus far Mn(III) derivatives have displayed limited reactivity toward the copolymerization of epoxides and CO_2 with the most active example being Inoue's (tpp)MnOAc catalyst in the presence of cyclohexene oxide.[17] Nevertheless, this system afforded low molecular weight copolymer with a TOF of only 16.3 h^{-1} at 80 °C, compared to ∼1200 h^{-1} under similar reaction conditions for (salen)CrX derivatives. The addition of good Lewis bases to the (tpp)MnOAc system was shown to inhibit catalytic activity, supportive of a second-order epoxide ring-opening mechanism where the epoxide binding site is blocked in this instance. In that same study, (salphen)MnOAc was ineffective toward formation of copolymer, producing instead only small quantities of poly(cyclohexene oxide).

Conclusions

Several (acacen)MnX complexes have been characterized crystallographically and their reactivity toward serving as

(52) (a) Darensbourg, D. J.; Mackiewicz, R. M.; Rodger, J. L.; Fang, C. C.; Billodeaux, D. R.; Reibenspies, J. H. *Inorg. Chem.* **2004**, *43*, 6024−6034. (b) Paddock, R. L.; Nguyen, S. T. *Macromolecules* **2005**, *38*, 6251−6253. (c) Luinstra, G. A.; Haas, G. R.; Molnar, F.; Bernhart, V.; Eberhardt, R.; Rieger, B. *Chem.−Eur. J.* **2005**, *11*, 6298−6314. (d) Cohen, C. T.; Coates, G. W. *J. Polym. Sci., Part A: Polym. Chem.* **2006**, *44*, 5182−5191.

(53) Boucher and Day have measured the magnetic moments for a variety of Mn(III) acacen complexes and found them to be high spin with values ranging from 4.30 to 5.09μ_B in both the solid state and solution.[18]

(54) Modification of the acacen ligand with CF_3 electron-withdrawing substituents significantly enhances the binding ability of a sixth ligand to the corresponding $Mn(III)N_3$ derivatives. These studies are currently underway in our laboratory.

catalysts for the copolymerization of cyclohexene oxide and carbon dioxide was evaluated. Although, in the solid-state the azide derivative, (acacen)MnN_3, exists as an extended polymer chain with the azide ligand spanning two manganese centers, in solutions of weakly interacting solvents (acacen)-MnN_3 is five-coordinate. The ν_{N3} stretching vibrational mode in this complex was employed to probe the ability of the manganese to bind a sixth ligand in solution, including anions, epoxides, and heterocyclic amines. This is made possible because the ν_{N3} stretch in (acacen)MnN_3 shifts to significantly lower frequency upon coordination of an additional axial ligand. The heterocyclic amine donors displayed greatly reduced binding ability in this instance compared to that seen in (salen)CrN_3, however, anions and epoxides displayed *no* inclination to bind as revealed by infrared spectroscopy. Concomitantly, these (acacen)MnX complexes exhibited very limited tendency to couple epoxides and CO_2 to afford copolymer or cyclic carbonate products.

Acknowledgment. We gratefully acknowledge the financial support from the National Science Foundation (CHE 05-43133) and the Robert A. Welch Foundation.

Supporting Information Available: X-ray crystallographic files in CIF format for the structure determinations of complexes **1**·$2H_2O$, **3**, **3′**, **3″**·(**3**·DMAP), **4**·EtOH, and **3**·pyr and a table listing the least-square plane analysis for the crystal structures. This material is available free of charge via the Internet at http://pubs.acs.org.

IC7003968